Rapid 3D Articular Cartilage Imaging with Reduction of Truncation Artifacts

R. Rakow-Penner[1], G. Gold[1], B. Daniel[1], J. Rosenberg[1], S. Mazin[1], J. Pauly[2], G. H. Glover[1]

[1]Radiology, Stanford University, Stanford, CA, United States, [2]Electrical Engineering, Stanford University, Stanford, CA, United States

Introduction: Three-dimensional knee MRI with spoiled gradient echo imaging (SPGR) is useful for cartilage volume and thickness measurements [1]. The long acquisition times of SPGR, however, limits its clinical use. This study demonstrates the clinical viability of an image processing technique [2] that can shorten 3-D real-time scanning by approximately 40%. The technique works by collecting fewer lines in the slice encode direction (kz), and then linearly predicting (LP) the uncollected lines up to the desired matrix size. Collecting fewer lines in the kz direction normally causes truncation artifacts from Gibbs ringing from the in-plane direction, and ghosting artifacts from adjacent images. In cartilage imaging, a tri-laminar appearance of cartilage has been noted as an effect of Gibbs ringing [3]. The LP method applied in this study reduces these 3D truncation artifacts. In this study, we show consistency of results and include statistics of radiologists' assessment of the images.

Methods: 3D data were collected on six knees at 1.5T (GE Healthcare, Waukesha, WI) using a dedicated receive-only knee coil (MRI Devices, Waukesha, WI). The knee protocol [4] includes: 3D fat-saturated SPGR, 50 slices/slab, 256x256, FOV 14 cm or 20 cm (depending on knee size), flip angle 10, BW +/-31.25kHz, TE 4.2ms, TR 20.7 ms. Full kz data was collected to provide a standard for ideal data. Truncation in the kz direction was followed by prediction that occurred in post processing. The data was truncated to 30 kz lines and then predicted back out to 50. Our method of LP is modified from Martin, et. al. [5] for 3D imaging. Our technique works in four steps. (1) K-space is multiplied by a ramp in the direction of truncation that weights k-space based on each line's distance from the origin. For our 3D application, x and y remain on one axis and are plotted against kz. Each kz line is then weighted accordingly. This now high-pass filtered data can more readily and accurately be used as inputs into a LP algorithm. (2) Each (x,y) line is independently autocorrelated in the kz direction. (3) These autocorrelated lines are then entered, along with the recursion order (number of previous kz lines used to predict the new line) into the Levinson-Durbin recursion algorithm. We used two different orders of recursion: 5 and 10. The recursion order is the number of previous kz lines that will be used in the calculation to predict the next line. We chose two different orders so that the radiologists could determine which they thought to be most efficient. The predicted kz lines are added to the original kz lines. (4) The ramp multiplied previous to prediction is divided out of all the data. Finally, kz is Fourier transformed into image space providing the augmented number of images.

To determine statistical significance of resultant images, two experienced radiologists reviewed five slices from each of the six knees. For each slice, four variations were presented at one time for scoring: (1) the gold standard of the full kz reconstructed image (2) the truncated kz reconstructed image without linear prediction (3) the LP image with recursion order = 5 and (4) the LP image with recursion order = 10. The images were randomly displayed for blinded review (Fig. 1). The radiologists were asked to score the image with the least artifact with a 10, the image with the most artifact with a 1 and to rank the two remaining images somewhere on that scale, allowing for ties. In addition, they were asked to determine the clinical acceptability of each image with a binary rating.

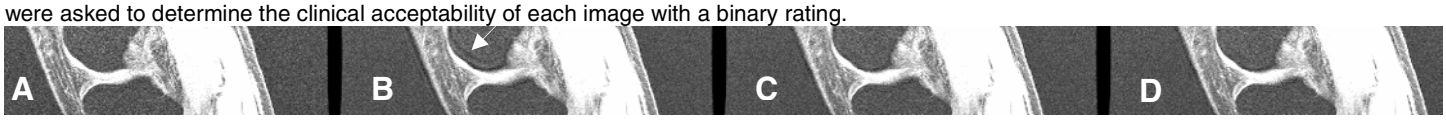

Figure 1. *Section through four sample images of the same knee. Radiologists were provided images of the entire knee. A section around the cartilage is shown above for emphasis. (A) Full kz image, used as gold standard (B) Truncated image without any correction. Notice ringing in the subchondral bone (arrow). (C) Linearly predicted image with recursion order = 5. (D) Linearly predicted image.*

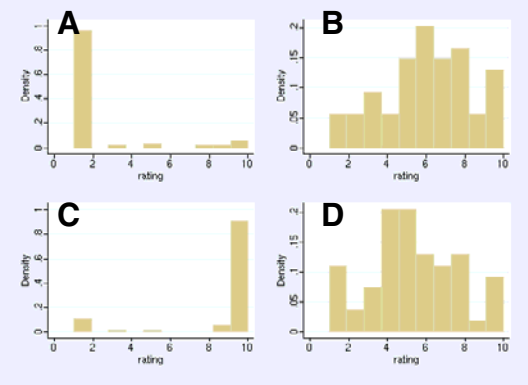

Figure 2. Histograms of pooled scoring for each of the 4 image variations. (A) Truncated, mean = 1.9, std. dev. = 2.4 (B) LP order 5, mean = 6.1, std. dev. = 2.5 (C) Gold standard, mean = 8.8, std. dev. = 2.9 (D) LP order 10, mean = 5.3, std. dev. = 2.5.

Results: Figure 2 presents histograms of the pooled ratings for each of the four image variations. A Wilcoxon signed-rank test demonstrated that the scores from the two LP variations (orders 5 and 10) were not significantly different from one another (p=0.16). However, they were both significantly different from the scores of the truncated images and the gold standard images (p<0.001). This indicates that the predicted images were better than the truncated images but not quite as good as the gold standard. A two-sided Fisher's exact test was used to evaluate the acceptability ratings. The acceptability of the gold standard images (with a pooled 93% acceptability rating) significantly differed from the truncated images (33% acceptability) with p<0.001. The gold standard images, the LP images with order 5 (95% acceptability), and the LP images with order 10 (78.3% acceptability) did not show a significant difference in acceptability (p= 1 for LP5 and gold standard, and p= 0.03 for LP10 and gold standard). The p-value for the LP order 10 verses gold standard images was relatively insignificant compared to the p-values < 0.001 that were calculated otherwise. The relative insignificance of this value compared to the obvious insignificance of the LP order 5 verses gold standard images highlights that the LP order 5 version may be the more robust variation. Overall, the acceptability statistics indicate that although the LP images may not be of the exact same quality as the gold standard, their quality is sufficient for diagnostic evaluation.

Conclusion: The linear prediction technique presented in this study allows for a 40% decrease in scan time, and sufficiently reduces truncation artifacts producing images acceptable for diagnostic evaluation. With shortened scan time, 3D SPGR articular cartilage imaging may become more clinically practical to conduct during limited scan times.

References: [1] Eckstein, et al. Ostearthritis and Cartilage. 10(12):922-928 (2002). [2] Rakow-Penner, et al. ISMRM Proceedings 2005, Abstract #2285. [3] Frank, et al. Am J Roentgenol. 168(2):547-554 (1997). [4] Gold, et. al. Radiographics. 23(5):1227:1242 (2003). [5]Martin, et al. J Magn Res. 82: 392-399 (1989). Funding provided by NIH P41-RR09784.